AN ABSTRACT OF THE THESIS OF

Emily Underwood for the degree of Master of Science in Geology presented on July 9, 2007.
Title: Sediment Transfer and Storage in Headwater Basins of the Oregon Coast Range: Transit times from ^{14}C Dated Deposits.

Abstract approved:

Stephen T. Lancaster

In steep headwater basins of the Oregon Coast Range (OCR), debris flows episodically deliver material from low-order tributary basins to larger catchments. Much of this material is stored in valleys and gradually removed by fluvial processes. Quantifying the transfer of material from hillslopes to mainstem channels is essential in understanding the routing of sediment through these headwater systems.

This study employs a dense radiocarbon sampling strategy to characterize the transit times of material delivered from tributaries to Cedar Creek and Golden Ridge Creek in the central OCR. As proxies for transit-times, sixty-eight age estimates from ^{14}C were removed from randomly assigned locations in the banks of tributary and mainstem channels at the channel confluences. Transit time distributions inferred from these age estimates have characteristic double-exponential shapes for both tributary deposits and imply mean transit times of 1240 ^{14}C yrs B.P. for Cedar and 1510 ^{14}C yrs B.P. for Golden Ridge Creek sites. This type of distribution indicates that younger deposits are preferentially evacuated such that, while most material moves through the tributary basins rapidly, there is a slower-moving component that can be stored in tributary deposits for millennia. Reservoir flux estimates derived from the inferred mean transit times indicate that most (>66%) of the sediment yield

of the Cedar Creek tributary is stored in the fan for some time but, for the Golden Ridge Creek deposit, only a small part (3%) of the basin tributary basin yield is stored there. These results indicate that debris fans similar to that at Cedar Creek play an important role in the transition between debris-flow and fluvial processes by buffering higher-order streams from episodic debris-flow inputs. In both cases, however, these depositional features retain effects of disturbance lasting for millennia.

Sediment Transfer and Storage in Headwater Basins of the Oregon Coast Range: Transit-times from ^{14}C Dated Deposits

by

Emily F. Underwood

A THESIS

submitted to

Oregon State University

in partial fulfillment of
the requirements for the
degree of

Master of Science

Presented July 9, 2007
Commencement June 2008

Master of Science thesis of Emily F. Underwood presented on July 9, 2007.

APPROVED:

Major Professor, representing Geology

Chair of the Department of Geosciences

Dean of the Graduate School

I understand that my thesis will become part of the permanent collection of Oregon State University libraries. My signature below authorizes release of my thesis to any reader upon request.

Emily F. Underwood, Author

ACKNOWLEDGEMENTS

The author expresses sincere appreciation to all who helped with this work. My advisor, Stephen Lancaster, provided me with ideas, support, funding, and advice without which this thesis would not have been possible. Andrew Meigs, Jay Noller, Gordon Grant and Fred Swanson contributed their extensive knowledge and teaching as well as valuable suggestions for the improvement of this project. Field work was greatly aided by Stephen Highland. Faron Anslow provided immensely helpful computing assistance and paleoclimatological insights. Discussions with John Henry clarified my understanding of probability distributions. Chris Gabrielli and Cheney Vidrine aided in the identification of charcoal samples.

TABLE OF CONTENTS

LIST OF FIGURES

Figure Page

LIST OF TABLES

Sediment Transfer and Storage in Headwater Basins of the Oregon Coast Range: Transit times from ^{14}C Dated Deposits

INTRODUCTION

Stream channel and valley morphology strongly reflect the balance of sediment supplied to a system and the ability of the stream to transport it (Sklar and Dietrich, 1998; Hancock and Anderson, 2002). When short-term sediment fluxes are equal to long-term denudation rates, landscapes are considered to be in a state of dynamic equilibrium, a concept firmly rooted in geomorphology (Gilbert, 1877; Hack, 1960; Reneau and Dietrich, 1991). When constructing sediment budgets and landscape evolution models for mountainous basins, streams are often assumed capable to transport all the sediment delivered to the fluvial system. Whereas this assumption may hold over geologic timescales, the short-term supply of sediment to a stream is typically not constant even where short-term sediment yields and long-term denudation rates are equivalent. This is particularly true in steep landscapes where debris flows intermittently deliver material to the fluvial system (Dietrich and Dunne, 1978, May and Gresswell, 2004). In these basins, sediment delivered to the channel episodically must be temporarily stored and gradually released by fluvial erosion. The sediment routing and storage processes that occur at the transition between debris-flow and fluvially dominated reaches are not well understood.

Prior studies in the steep, rugged slopes and deeply dissected valleys of the Oregon Coast Range (OCR) have provided insight into the routing and storage of sediment in headwater landscapes (Dietrich and Dunne, 1978; Reneau et al., 1989; Benda and Dunne, 1997; Lancaster et al., 2001). In unchanneled hollows of the OCR, gradual soil creep and episodic debris flows triggered by shallow landslides (Montgomery and Dietrich, 1994; Iverson et al., 1997) constitute the dominant modes

of sediment delivery to the fluvial system (Reneau and Dietrich, 1991). These debris flows scour channels to bedrock, entraining additional material as they travel (Stock and Dietrich, 2003). In the Pacific Northwest, a major component of debris flow material is wood, constituting on average 60% of debris flow volume (Lancaster et al., 2003). These woody debris flows typically stop upon arrival at channel junctions or areas where gradients decrease (Benda and Cundy, 1990) and form dams that impound sediment and subsequent debris flows (Lancaster and Grant, 2006). This mechanism delivers sediment to the system in episodic pulses, which are then gradually eroded by fluvial processes. Studies in the OCR indicate that long term denudation rates are approximately equivalent to short term sediment yields, implying landscape equilibrium (Reneau and Dietrich, 1991; Heimsath et al. 2001). This equivalence suggests that transitional headwater zones store episodic inputs of sediments from debris flows. Dietrich and Dunne (1978) illustrate this concept with an example from the floods of 1964-65, which discharged an estimated 10,000 tons of sediment in the 16 km^2 Rock Creek basin in the OCR. This volume is comparable to twenty years of creep discharge for the watershed, yet the sediment yield from the basin was much lower due to the storage of much of this sediment in tributary fans and channels at the transition between debris-flow and fluvial processes.

This time lag between sediment delivery and removal in these steep basins complicates our understanding of the transfer of material from hillslopes to the fluvial system. What are the primary features in headwater landscapes that store sediment? How long does it take for sediment to move from hillslopes to the fluvial system?

One approach to addressing these questions is to identify the various storage reservoirs in a basin and quantify their sediment routing characteristics. Age distributions of the sediment in various basin deposits provide information about the time required for the evacuation of sediment from these reservoirs (Dietrich et al., 1982). Bolin and Rhode (1973) show how the transit-time distributions of particles in a reservoir provide information about the processes which transport material into and out of that reservoir. It is important to note some discrepancies in the literature regarding reservoir terminology. Bolin and Rhode (1973) use the terms "residence time" and "average transit time" to refer to the age of particles leaving the reservoir, and the term "average age" for the average age of material within the reservoir. Ericksson (1971) uses the term "turnover time" to refer to the mean age of material leaving a reservoir, and the term "residence time" to refer to the average age of material in the reservoir. In the case of a perfectly mixed reservoir, all of these terms are equal. This discussion will use the theoretical framework and terminology of Bolin and Rhode (1973) who illustrate different types of reservoirs based on the relationship between the average age and average transit time of material in the reservoir.

This study develops a methodology for the purpose of characterizing the *transit times* of sediment reservoirs. It is helpful to visualize a simple vat with an inlet and an outlet (Figure 1). When material enters the reservoir, it has a transit time of zero. Each component exiting the reservoir has spent some amount of time in the vat, the transit time. Material exiting the reservoir can have a range of transit times depending on the manner in which material moves through the vat. For so-called

plug flow, a transit-time distribution is centered about a non-zero peak, and the average age of material is less than the transit time because the material leaving the reservoir is the oldest. In a perfectly mixed reservoir, all material has an equal likelihood of being evacuated, regardless of when it entered, so the average transit time and the average age are equal. In this case, both transit-time and age distributions are represented by exponentials. In a third case, most material entering the reservoir evacuates quickly so that the average transit time small. However, the material that stays longer remains in the reservoir for long enough to make the average age relatively large. In this situation, the transit-time distribution might resemble a double-exponential with one decay scale much shorter than the other. The associated age distribution has a larger concentration of old material, relative to a perfectly-mixed reservoir.

Applying this conceptual framework to a sediment reservoir requires a definition of an "outlet" and some tracer that captures transit times of material exiting the reservoir. For material in valley-bottom or fan storage, material in the banks of channels is the most likely to be removed. If the average transit time within the channel is much less than the average transit time in storage, then the ages of material in those banks are proxies for transit times. We assume that in-channel transit times are much less than transit times in off-channel storage. Fragments of detrital charcoal and wood found in these banks therefore serve as a tracer that can be dated using radiocarbon techniques. In this way, collecting material from channel banks is analogous to standing at the outlet of the reservoir with a bucket gathering material leaving the reservoir.

In a preceding study using this conceptual framework (Lancaster and Casebeer, in press), radiocarbon samples were obtained from two adjacent reaches of the mainstem of Bear Creek, a 2.23 km^2 basin in the OCR. The inferred average transit time (residence time) for the debris-flow dominated upper reach (440 ^{14}C yrs. B.P.) is significantly lower than that for the lower, fluvially dominated reach (1220 ^{14}C yrs. B.P.). Perhaps more interesting is that the inferred transit time distributions of the two reaches are distinctly different. The transit time distribution for the lower reach is best fit by an exponential, whereas the upper reach transit times are better fit by a power law. This difference implies that the lower, fluvially dominated reach acts like a fully-mixed reservoir. In other words, all sediments have an equal probability of evacuation, regardless of age. The "mixing" here results from change in the position of the channel on the valley floor rather than the actual mixing of the sediments. Transport in the upper reach is dominated by debris flows which preferentially evacuate younger material, leaving older sediments to linger.

In this study employs a spatially-dense, volume-weighted, radiocarbon dating strategy in order to assess sediment storage characteristics of headwater catchments in the OCR. This study focuses on two tributary confluence deposits occurring atop strath terraces above the main channel. The distributions of radiocarbon dates from these deposits provide a quantification of transit times of material through these depositional features.

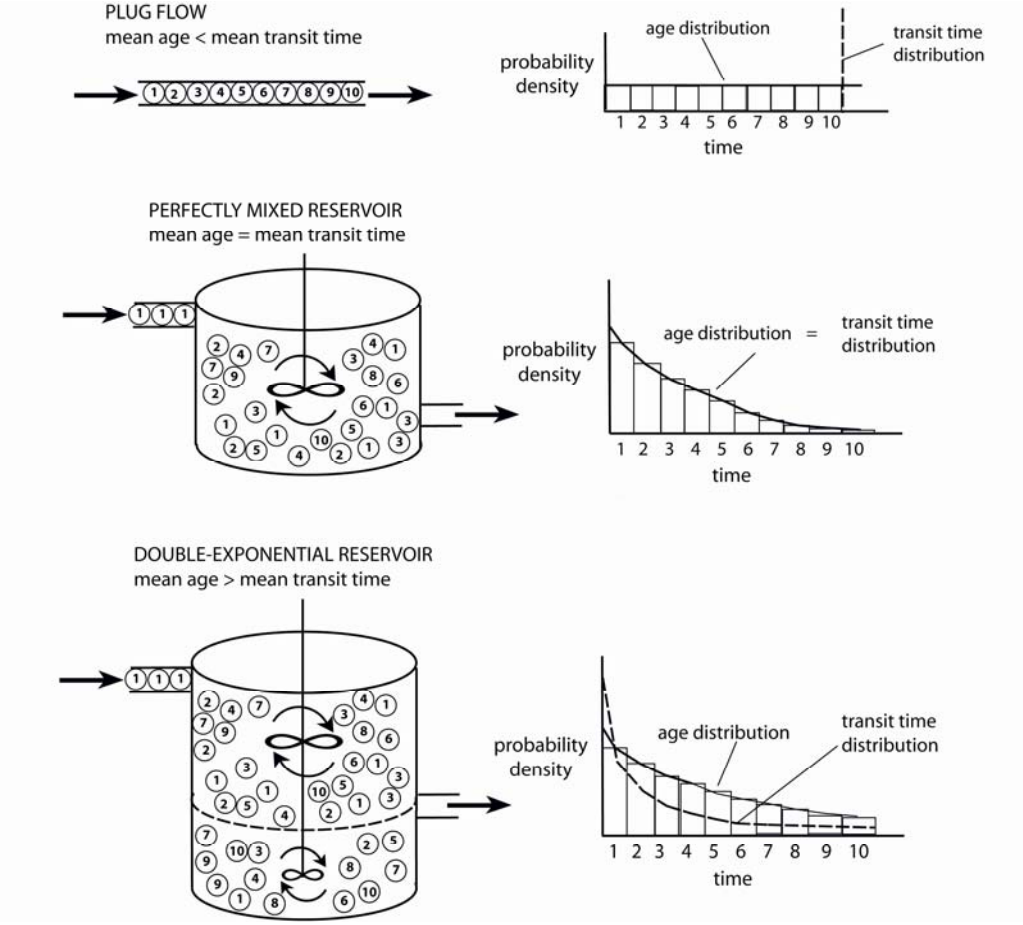

Figure 1. Conceptual diagram illustrating how age distributions and transit time distributions reflect reservoir characteristics. Material entering each reservoir has an age of 1. Material exiting the reservoir has transit times of 1 through 10, indicating the amount of time that component resided in the reservoir. Transit time distributions show the age of material collected at the outlet. Age distributions represent the age of all the material contained within the reservoir.

STUDY AREA IN THE OREGON COAST RANGE

In the Oregon Coast Range, our study sites are located within the Tyee Formation, which consists of thickly bedded Eocene turbidite deposits with local igneous intrusions (Heller and Dickinson, 1985). Subduction of the Juan de Fuca Plate has resulted in regional uplift since the Miocene (Kelsey et al., 1996). The terrain of the OCR is steep and highly dissected with ridge lines of relatively uniform elevation of about 500 meters. Hillslope soil cover is typically thin (~ 0.5 meters) (Dietrich and Dunne, 1978; Heimsath et al. 2001). There is no geomorphic expression of glacial processes, due to an absence of glaciation in the OCR during the Pleistocene (Baldwin, 1993). The region is thickly forested by large conifers [Douglas fir (*Pseudotsuga menziesii*), western hemlock (*Tsuga heterophylla*), western red cedar (*Thuja plicata*)], and some hardwoods [red alder (*Alnus rubra*), and big leaf maple (*Acer macrophyllum*)] especially in riparian zones. Cool, wet winters and warm, dry summers characterize the present climate of the OCR. Long-duration rainstorms predominately occurring from October to May combine with steep, high relief slopes produce debris flows, typically where the roots of the dense forest have been weakened by tree mortality (Montgomery et al., 2000).

The two study sites are tributary junctions where strath terraces are overlain by thick deposits with terrace risers bordering the channel. The first site is a debris fan on Cedar Creek, a 6.8 km^2 tributary basin of Sweet Creek, which drains into the Siuslaw River (Figures 2 and 3). The mainstem contributing area at this tributary junction is 4.8 km^2. A right bank-tributary with a contributing area of 0.14 km^2 feeds the fan (Table 1). This channel splits into two main distributary channels which have

incised the distal fan to bedrock. The second site is a tributary junction in Golden Ridge Creek, tributary of Wassen Creek and eventually the Smith River (Figure 2). The strath terrace occurs at the outlet of a 1.5 km^2 left-bank tributary (mainstem contributing area 6.3 km^2), about one kilometer upstream of the confluence of Golden Ridge Creek and Wassen Creek (Table 1). Approximately four meters of sandy alluvium overlie a strath terrace at the outlet of the tributary. The tributary channel has incised through these deposits to bedrock. An important difference between these sites is that the Cedar Creek deposits are primarily of debris flow origin, and the Golden Ridge Creek deposits are comprised of fine alluvial material.

Table1. Characteristics of mainstem and tributary features at Cedar Creek and Golden Ridge Creek study sites.

Site Characteristics	Terrace/Tributary		Mainstem	
	Cedar Creek	Golden Ridge Creek	Cedar Creek	Golden Ridge Creek
Channel gradient	9.8E-02	4.8E-02	4.7E-02	3.1E-02
Valley gradient	-	-	5.0E-02	3.5E-02
Deposit volume (m^3)	3.6E+04	3.2E+03	6.9E+03	9.8E+02
Contributing area (km^2)	0.14	1.5	4.8	6.3
bulk density (g/cm^3)	1.1 ± 0.3	1.2 ± 0.3	1.3 ± 0.3	1.7 ± 0.2
mass of deposits (kg)	4.2.E+07	3.9.E+06	9.1E+06	1.7E+06
average transit time (^{14}C yrs B.P.)	1240 ± 1995	1510 ± 1790	410 ± 520	1370 ± 5620
flux through reservoir (kg/yr)	3.4E+04	2.5E+03	2.2E+04	5.1E+02
basin yield (kg/yr)	3.2E+04	3.4E+05	1.1E+06	1.4E+06
% of denudation stored	1.1	7E-03	2.0E-02	3.5E-04

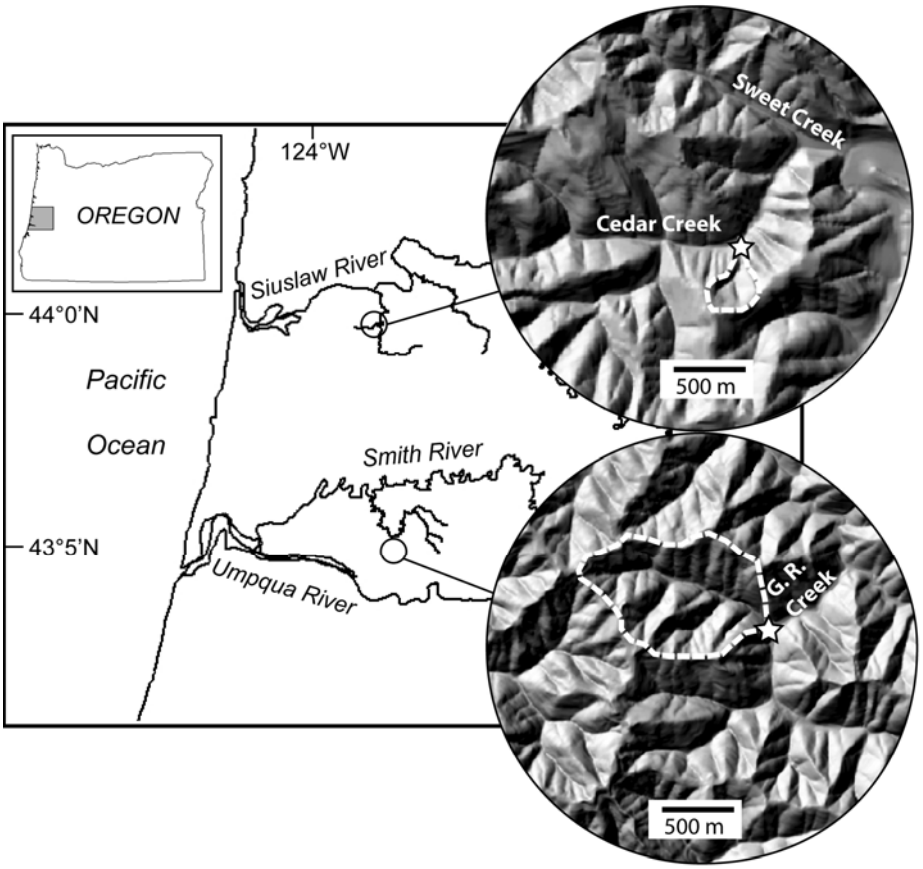

Figure 2. Location map of the Cedar and Golden Ridge (G.R.) Creek study sites in the central Oregon Coast Range. Dashed white lines outline contributing tributary basins in the insets. Stars indicate the location of the sampled tributary deposits.

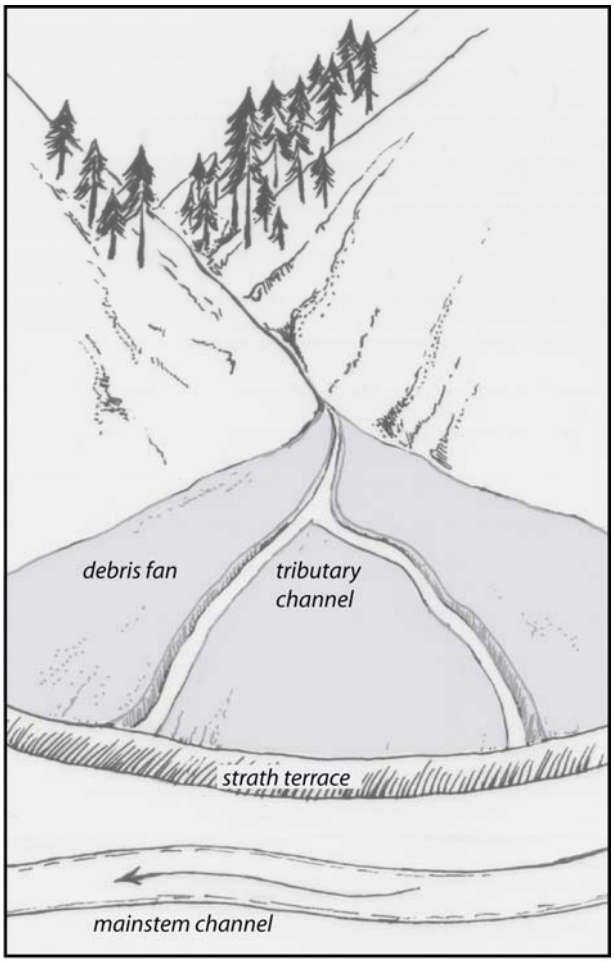

Figure 3. Idealized drawing illustrating relative orientations of tributary, debris fan, strath terrace and main channel at Cedar Creek site.

METHODS

Radiocarbon sampling strategy

The construction of transit time distributions from bank material requires a volume-weighted sampling strategy that is not biased by over-sampling "interesting" (often old-looking) deposits. For this reason, a dense, random, volume-weighted sampling strategy was employed which differs from more conventional radiocarbon sampling strategies. For example, Meyer et al. (1995) used a dense radiocarbon sampling strategy to investigate depositional patterns on alluvial fans in Wyoming. Radiocarbon samples were removed from discrete sedimentary layers, often related to individual fire events and subsequent debris flows. In the OCR, Personius et al. (1993) extracted radiocarbon samples from the alluvial tread overlying strath terraces in order to constrain the timing of abandonment. In this study, the radiocarbon sample locations were assigned *before* characterization of the deposits. By sampling this way, the array of radiocarbon ages represents the entire deposit, not just remarkable strata.

Deposit Volumes and Sample Locations

In order to develop a volume-weighted sampling strategy, the geometries of the sediment stored at each site were first determined. At the Cedar Creek site, the longitudinal profiles of the main and tributary channels were surveyed with tape, compass, stadia rod, and hand level. To constrain the volume of the debris fan and adjacent channel deposits, four valley-spanning transects were surveyed, two converging at the fan apex and the others at the upstream and downstream ends of the fan. Measurement of the bedrock strath terrace elevation at several points allowed for

the calculation of its slope and the construction of a plane defining the lower boundary of the fan volume. Similarly, the valley gradient defined the slope of a plane setting the lower boundary of the mainstem deposits. The lateral dimensions of the fan were calculated by assuming 40º valley walls extended beneath the fan surface. A rectangle encompassing the total volume of the fan, channel, and floodplain deposits was then populated with random coordinates. (The term "floodplain deposits" is used to indicate valley floor deposits adjacent to the mainstem channel.) Points which were not contained within the fan or channel deposits were eliminated (Figure 4).

The survey strategy for the Golden Ridge Creek site differed slightly due to a different geometry. Four parallel transects encompassing the terrace deposits and the adjacent floodplain deposits were surveyed on both the mainstem and tributary channels. The volume of the valley bottom sediment was then determined and populated with random sample coordinates. The total number of radiocarbon samples was divided among the tributary and mainstem deposits relative to their volume.

At each site the location of each sample point was projected to the nearest bank and matched to the tape distance along the channel surveys. The vertical height of each sample location was related to a height in the channel bank by subtracting elevation of the channel bed from the sample location elevation. At each sample location the bank was excavated with a shovel to obtain a fresh exposure. This excavation also allowed characterization of the deposit and inference of the mechanism of deposition following Collinson (1978): sorted, rounded, clast-supported gravels suggest high-energy fluvial deposition; fine sedimentary layers

interbedded with organic material indicate low-energy fluvial deposition; and poorly sorted, angular, matrix-supported clasts characterize debris flow deposition. Each deposit was classified either as a debris flow deposit, fluvial gravels, or fluvial fines. This classification scheme can be somewhat problematic, as fluidized debris flows can produce sedimentary facies that are well-sorted and matrix-poor (Suwa and Okuda, 1983; Major, 1997) and thus can be easily mistaken for a fluvial deposit, particularly if the deposit contains reworked rounded fluvial material. Also, some debris flow deposits have been subsequently reworked by fluvial processes, further complicating this type of classification. A deposit was classified as fluvial if it showed evidence of fluvial deposition such as imbrication or stratification. After characterization of the bank material, the sample height was measured from the thalweg of the channel. Radiocarbon-datable material was then found in this location by digging laterally into the bank. If the sample location was obstructed by a boulder or log, the sample was taken from either the opposite bank or from the nearest sediments allowing feasible sampling (always within a meter of the original point). Care was taken to avoid taking samples from areas that were obviously bioturbated (burrows, roots, etc). Dateable material was found at all sample points, and therefore the sampling was not biased by the absence of old material. Samples were closely inspected to identify characteristic features that allowed species classification (cell structure, resin canals, earlywood/latewood transition, spiral thickenings; Hoadley, 1990).

The samples were analyzed at the Accelerator Mass Spectrometer facility at the University of Arizona. The resulting radiocarbon age estimates were calibrated

using the OxCal program (Bronk Ramsey, 2001) with the Int-Cal04 and BombNH04 calibration curves (Reimer et al., 2004; Hua and Barbetti, 2004). The resulting probabilities were summed and normalized for each of the terrace and mainstem deposits to provide relative probability densities of sample age estimates and, thus, inferred transit-time distributions.

Bulk Densities

Sediment samples were taken at every third sample location with a soil probe, perpendicular to the bank. These samples were dried and weighed to determine dry bulk densities. Because the sample diameter was limited to 5 centimeters, larger grain sizes were not sampled, and bulk densities may represent minimum estimates.

Exceedance Distributions

Plotting the radiocarbon ages as exceedance distributions allows inference of reservoir characteristics. The exceedance distribution shows the probability of transit times greater than or equal to time, τ. For the purpose of characterizing the *shapes* of these distributions, the calibrated ages are unwieldy the uncalibrated ^{14}C ages are used to construct the plots. Functions were fit to the exceedance distributions in order to characterize their shapes and, from those shapes, infer reservoir characteristics (Figure 1).

Reservoir Fluxes

Bolin and Rhode (1973) show that for a steady-state reservoir the transit time (τ_t) of particles leaving a reservoir is equal to its turnover time (τ_o), which is given by:

$$\tau_o = M_o / F_o \quad (1)$$

where M_o is the total mass of the reservoir and F_o is the total flux rate through the reservoir. By assuming steady-state conditions, the long-term flux through the reservoir can be solved by using the mean radiocarbon age of bank deposits as a proxy for the mean transit time. This assumption is reasonable over millennial timescales in which the total volume of material stored has not changed drastically. This analysis also requires the assumption that the radiocarbon ages represent the timing of deposition at the tributary confluence. The suitability of this assumption will be discussed in later sections. The mass of each fan is determined by multiplying surveyed volume by average measured bulk densities.

Calculating a basin flux allows comparison of the quantity of material passing through a reservoir to the amount produced by the contributing basin. By assuming a uniform denudation rate of 0.1 mm/yr (Heimsath et al., 2001) over the contributing area and a weathered rock density of 2270 kg/m^3 (Anderson, 2002), allows calculation of the basin flux.

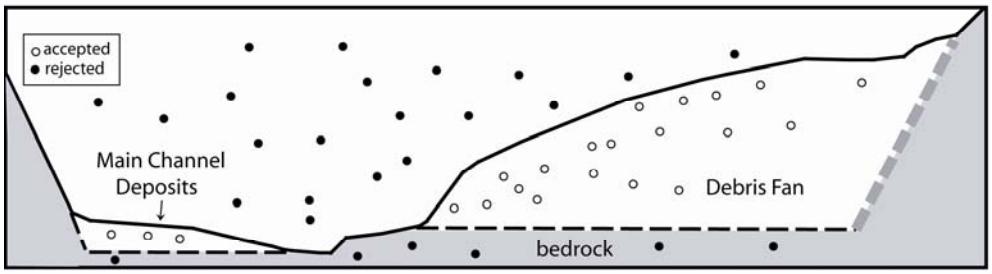

Figure 4. Diagram showing surveyed cross-section of tributary and mainstem deposits with hypothetical randomly generated coordinates within a rectangular space. Sample locations that do not fall into the tributary or mainstem deposits are rejected. Additionally samples located an unfeasible sampling distance below the tributary channel bed were also rejected. The remaining samples are projected to the nearest tributary or mainstem channel bank.

RESULTS

AMS Age Estimates

The uncalibrated AMS radiocarbon ages and calibrated ranges are shown in Table 2. Figures 5 and 6 show the distribution of the sample locations in plan view. At the Cedar Creek site, thirty samples were taken from the fan, twenty-one of which were taken from banks classified as debris-flow deposits. Eight deposits were classified as fluvial gravels, and one was classified as fluvial fines. The samples removed from fluvial deposits are generally younger than those removed from debris-flow deposits. The fan samples have a mean uncalibrated radiocarbon age of 1240 ± 1995 ^{14}C yrs. The five samples from the adjacent channel deposits have a mean age of 410 ± 520 ^{14}C yrs. Two of these samples were removed from one debris-flow deposit and the remaining three from fluvial deposits. At the Golden Ridge Creek site, twenty-four samples were taken from fluvial fines and fluvial gravels overlying the strath terrace (there were no debris flow deposits).The mean uncalibrated radiocarbon age of these samples is 1510 ± 1790 ^{14}C yrs. Eight fluvial deposits were sampled in the main channel and had a mean age of 1370 ± 5620 yrs. Two of these samples returned exceptionally old ages, (10,760 ^{14}C yrs B.P. and 13,790 ^{14}C yrs B.P.) The probability distributions of the calibrated ages are shown in Figure 7, 8, and 9. Note that calibrated radiocarbon ages typically have multiple likely ages and exhibit asymmetry. This is a result of fluctuations in the atmospheric ^{14}C content reflected in the calibration curve. A peak in the distribution does not represent a single date, but rather the probability that one or more samples is of that age.

Exceedance Distributions

The exceedance plots of transit times (Figure 10) can be compared to theoretical transit time distributions for various types of reservoirs. For both fans, the radiocarbon ages are clearly peaked at zero, so a plug-flow transport model (Figure 1) does not apply. The distributions for both fans are poorly fit by exponentials (the sample standard deviations are larger than the sample means) and suggest that sediment in these reservoirs is not "well-mixed". Rather, the probability of evacuation is age-dependent. Bolin and Rhode (1973) describe a case where the average age of the elements in a reservoir is greater than the average transit time. In such a situation the transit time distribution, $\varphi(\tau)$, is a double exponential function given by

$$\varphi(\tau) = Ae^{-\alpha\tau} + (1-A)e^{-\beta\tau} \qquad (2)$$

Both deposits are well fit by this function. Note that the raw ages are shifted so that the minimum age for each deposit is zero. Although the deposit distributions are peaked at the youngest ages, neither deposit returned samples with ages much less than 100 years. Due to this lack of very young material, fitting exponential distributions to the *unshifted* dates produces a fit that is greater than one at zero age. Setting the youngest date equal to zero allows a fit to the probability distribution that equals one at zero.

The mainstem exceedance distributions are shown in figure 11. Due to the small number of samples, no fits are given for these data.

Deposit Volumes and Reservoir Fluxes

The deposit volumes, deposit bulk densities, masses, reservoir fluxes, and basin yields are given in Table 1. The ratios of the reservoir fluxes to the basin yields are also given.

Table 2. Radiocarbon sample locations and ages

Sample	Lab no.	Loc.*	Dis.† (m)	B§	Ht.# (m)	Dep**	^{14}C age (BP)	calibrated age	Sample des. ††
CCC-1	AA71597	Cedar	78	L	0.72	FG	1345 ± 45	616-773	w/c, *p.m.*
CCC-2	AA71612	Cedar	108	L	0.69	DF	170 ± 35	1660-1954	c, *p. m.*
CCC-3	AA71613	Cedar	108	L	0.19	DF	180 ± 35	1652-1954	c
CCC-4	AA71604	Cedar	123	L	1.77	FF	155 ± 35	1665-1953	p.b.b.
CCC-5	AA71629	Cedar	36	R	0.03	FG	225 ± 35	1527-1955	p.b.b.
CCF-1	AA71624	C1282R	41	L	2.65	DF	2500 ± 35	790-421 B.C.	c
CCF-2	AA71628	C1282R	69	L	2.3	DF	190 ± 35	1213- 1955	c, *p. m.*
CCF-3	AA71630	C1282R	31	R	0.35	DF	670 ± 40	1270-1395	c, *p. m.*
CCF-4	AA71621	C1282R	65	L	1.73	DF	3235 ± 40	1610-1430 B.C.	c
CCF-5	AA71620	C1282R	72	R	0.89	DF	520 ± 35	1320-1445	c, ≠ *p. m.*
CCF-6	AA71619	C1282R	69	L	1.75	DF	430 ± 35	1418-1618	c, b.
CCF-7	AA71618	C1282R	63	R	2.75	DF	2960 ± 35	1304-1051 B.C.	c, *p. m.*
CCF-8	AA71617	C1282R	38	R	0.88	DF	105 ± 35	1680-1939	c, *p. m.*
CCF-9	AA71623	C1282R	25	L	0.45	FG	195 ± 40	1343-1955	c
CCF-10	AA71606	C1282R	100	R	0.81	DF	130 ± 40	1669-1944	w/c, *p. m.*
CCF-11	AA71608	C1282R	32	L	1.73	DF	195 ± 40	1644-1955	p.b.b.
CCF-12	AA71607	C1282R	63	L	1.36	DF	135 ± 35	1669-1945	c
CCF-13	AA71610	C1282R	61	L	2.04	DF	215 ± 35	1641-1955	w/c, ≠ *p. m.*
CCF-14	AA71602	C1282R	49	R	2.53	DF	270 ± 35	1494-1953	c, *p. m.*
CCF-15	AA71615	C1282R	69	R	0.19	DF	960 ± 40	995-1170	c
CCF-16	AA71609	C1282R	69	R	0.95	DF	575 ± 40	1298-1425	c
CCF-17	AA71605	C1282R	65	L	1.21	FG	235 ± 40	1520-1955	c, *p. m.*
CCF-18	AA71598	C1282R	67	L	0.68	DF	2040 ± 40	166 B.C. -52	c, *p. m.*
CCF-19	AA71599	C1282R	41	L	3.47	DF	1535 ± 40	427-601	c
CCF-20	AA71616	C1282R	29	L	0.26	FG	910 ± 60	1018-1251	c
CCF-21	AA71614	C1262R	17	L	3.56	DF	5935 ± 50	4939-4715 B.C.	c
CCF-22	AA71611	C1262R	24	L	3.07	DF	2075 ± 40	197 B.C. -4	c, *p. m.*
CCF-23	AA71622	C1262R	51	L	0.55	DF	445 ± 35	1412 -1612	c, ≠ *p. m.*
CCF-24	AA71603	C1262R	27	R	-0.66	FG	255 ± 35	1515-1954	c, *p. m.*
CCF-25	AA71601	C1262R	10	L	-0.41	FG	695 ± 50	1224 -1394	c, *p. m.*
CCF-26	AA71600	C1262R	16	R	-0.05	FF	100 ± 40	1680-1939	c
CCF-27	AA71627	C1262R	12	L	-0.49	FG	225 ± 30	1639 -1955	w
CCF-28	AA71625	C1282R	68	R	-0.41	DF	180 ± 35	1649-1954	c
CCF-29	AA71626	C1282R	19	R	1.42	DF	9295 ± 55	8705-8337B.C.	c
CCF-30	AA71631	C1262R	6	R	0.03	FG	95 ± 40	1680-1939	p.b.b.

Table 2 (continued)

Sample	Lab no.	Loc.*	Dis.† (m)	B§	Ht.# (m)	Dep**	^{14}C age (BP)		calibrated age	Sample des.††
T8-1	AA72008	T-2	6.3	L	1.58	FG	400 ±	35	1436-1631	c,b.
T8-2	AA72007	T-1	16.6	R	0.77	FF	745 ±	35	1401-1470	c, *p. m.*
T8-3	AA72006	T-1	26.6	R	0.35	FF	1010 ±	35	902 -1153	c
T8-4	AA72005	T-2	5.1	L	0.68	FG	975 ±	35	997-1155	c, *p. m.*
T8-5	AA72004	T-2	5.4	L	2.88	FF	910 ±	35	1032-1209	c, *p. m.*
T8-6	AA72003	T-2	17.6	L	2.88	FF	130 ±	35	1670-1943	c
T8-7	AA72002	T-2	11.6	R	3.06	FG	480 ±	35	1400-1467	c
T8-8	AA72001	T-2	36.0	R	0.15	FG	5,000 ±	45	3944-3671 B.C.	c
T8-10	AA72000	T-2	39.6	R	0.67	FF	1,270 ±	35	664 -865	c, *p. m.*
T8-11	AA71999	T-2	11.0	L	3.48	FG	4,700 ±	60	3635-3367 B.C.	c
T8-12	AA71998	T-2	14.4	R	2.36	FG	230 ±	40	1521-1955	p.b.b.
T8-13	AA71997	T-2	21.8	L	2.11	FF	690 ±	45	1252-1398	c, ≠ *p. m.*
T8-14	AA71996	T-2	21.2	L	2.38	FG	2,195 ±	35	375-175 B.C.	c, ≠ *p. m.*
T8-15	AA71995	T-1	14.7	R	1.06	FF	855 ±	33	1048-1261	c
T8-16	AA71994	T-2	18.3	L	3.11	FF	195 ±	33	1646-1955	c
T8-17	AA71993	T-2	12.9	L	1.49	FG	6,140 ±	40	5215-4964 B.C.	c, ≠ *p. m.*
T8-18	AA71992	T-1	6.5	R	0.4	FG	1,070 ±	35	895-1022	c
T8-19	AA71991	T-2	36.6	L	1.05	FG	5,070 ±	40	3963-3782 B.C.	c
T8-20	AA71990	T-1	28.8	L	0.12	FF	210 ±	30	1643-1955	c, *p. m.*
T8-21	AA71989	T-1	28.8	R	0.48	FF	1,950 ±	35	37 B.C. -126	c
T8-22	AA71988	T-2	30.2	L	2.09	FG	845 ±	35	1050-1264	c, *p. m.*
T8-23	AA71987	T-0	19.6	R	0.05	FF	370 ±	35	1446-1634	c, *p. m.*
T8-24	AA71986	T-2	14.6	R	2.56	FG	530 ±	35	1319-1442	c
T8-25	AA71985	T-2	9.0	R	2.44	FG	390 ±	35	1441-1633	c, *p. m.*
GRC-1	AA72016	GRC	21.3	R	0.17	FG	180 ±	35	1648-1955	c
GRC-2	AA72015	GRC	39.8	L	0.62	FF	215 ±	35	1640-1955	w/c
GRC-3	AA72014	GRC	36.1	L	0.1	FG	13,790 ±	850	16864-12294 B.C.	c
GRC-4	AA72013	GRC	38.0	L	0.44	FG	150 ±	35	1667-1951	c
GRC-5	AA72012	GRC	14.4	R	0.83	FG	175 ±	35	1654-1954	c, *p. m.*
GRC-6	AA72011	GRC	-8.0	L	0.49	FF	870 ±	35	1044-1253	c/w
GRC-7	AA72010	GRC	6.1	R	0.39	FG	10,760 ±	620	12091-8836 B.C.	c, ≠ *p. m.*
GRC-8	AA72009	GRC	44.8	R	0.97	FG	post-bomb§§		1953-1956	c

*Loc.= channel from which sample was removed. Cedar= mainstem channel, C1262R= downstream tributary channel, C1282R= upstream tributary channel.

†Dis.= surveyed tape distance along channel.

§B= bank from which sample was removed, R=right bank, L=left bank.

Ht.= height above channel thalweg, negative heights indicate that sample was removed from below the channel bed.

**Dep.= type of deposit from which sample was removed. DF=debris-flow deposits, FG= fluvial gravels, and FF= fluvial fines.

††Sample desc.= sample description. c= charcoal, w=wood, w/c= partially burnt wood, b.=bark, p.b.b.=partially burnt bark, *p.m.*= *psuedotsuga menziesii*, ≠ *p. m.*= not *psuedotsuga menziesii*

§§ fraction of modern = 1.0160 ± 0.0042

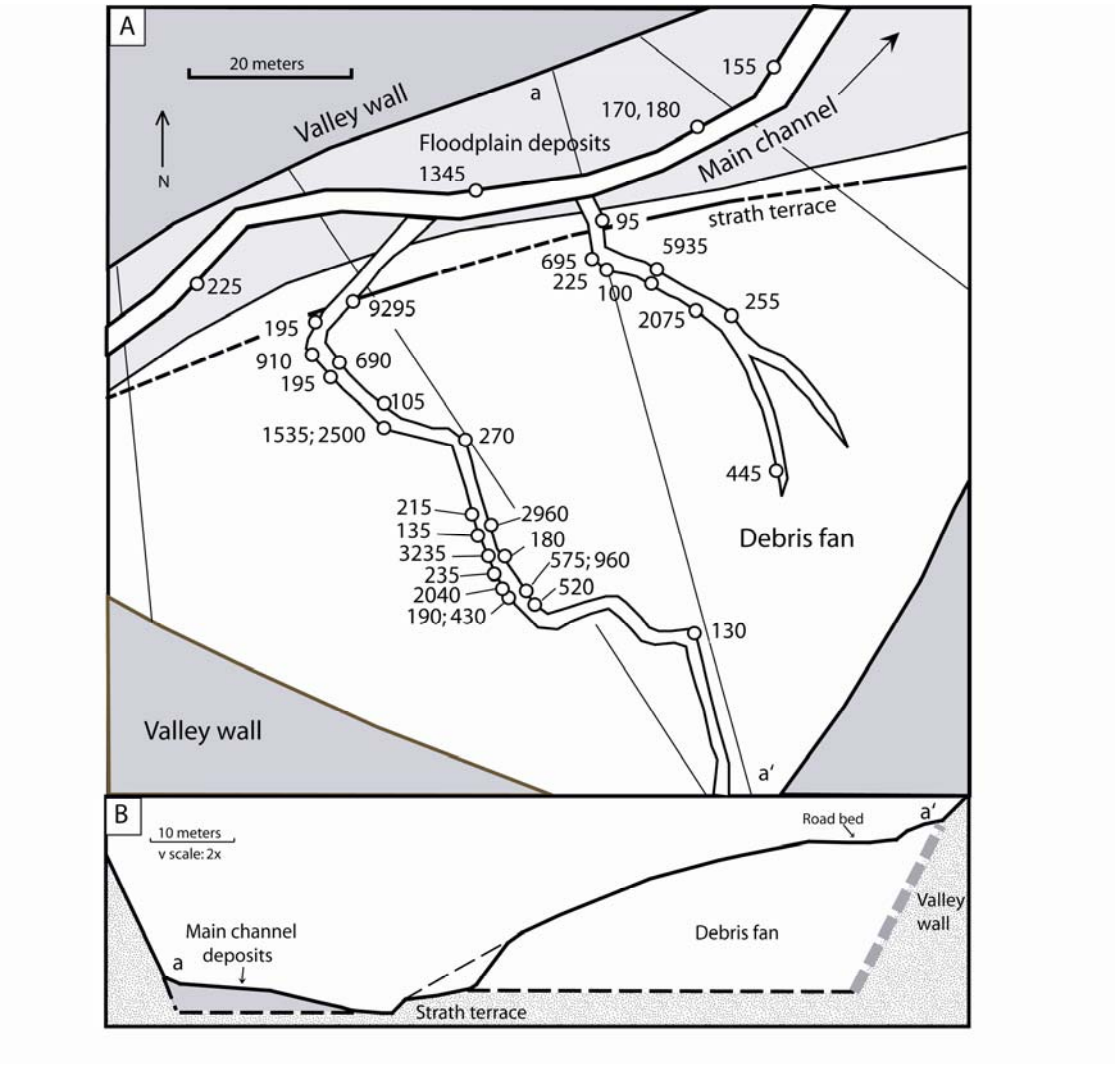

Figure 5. Map of Cedar Creek Site with radiocarbon age estimates. (A) Plan view of Cedar Creek study site. Surveyed mainstem and tributary channels and surveyed transects are shown with the locations of sampled deposits. Numbers indicate the raw radiocarbon ages (^{14}C yrs. B.P.). 1σ error is less than 100 ^{14}C yrs B.P. for all age estimates (Table 2). (B) Cross sectional map based on cross-valley survey of fan surface from a to a'. Dashed lines indicate interpreted bedrock geometry. Thin dashed line indicates fan surface.

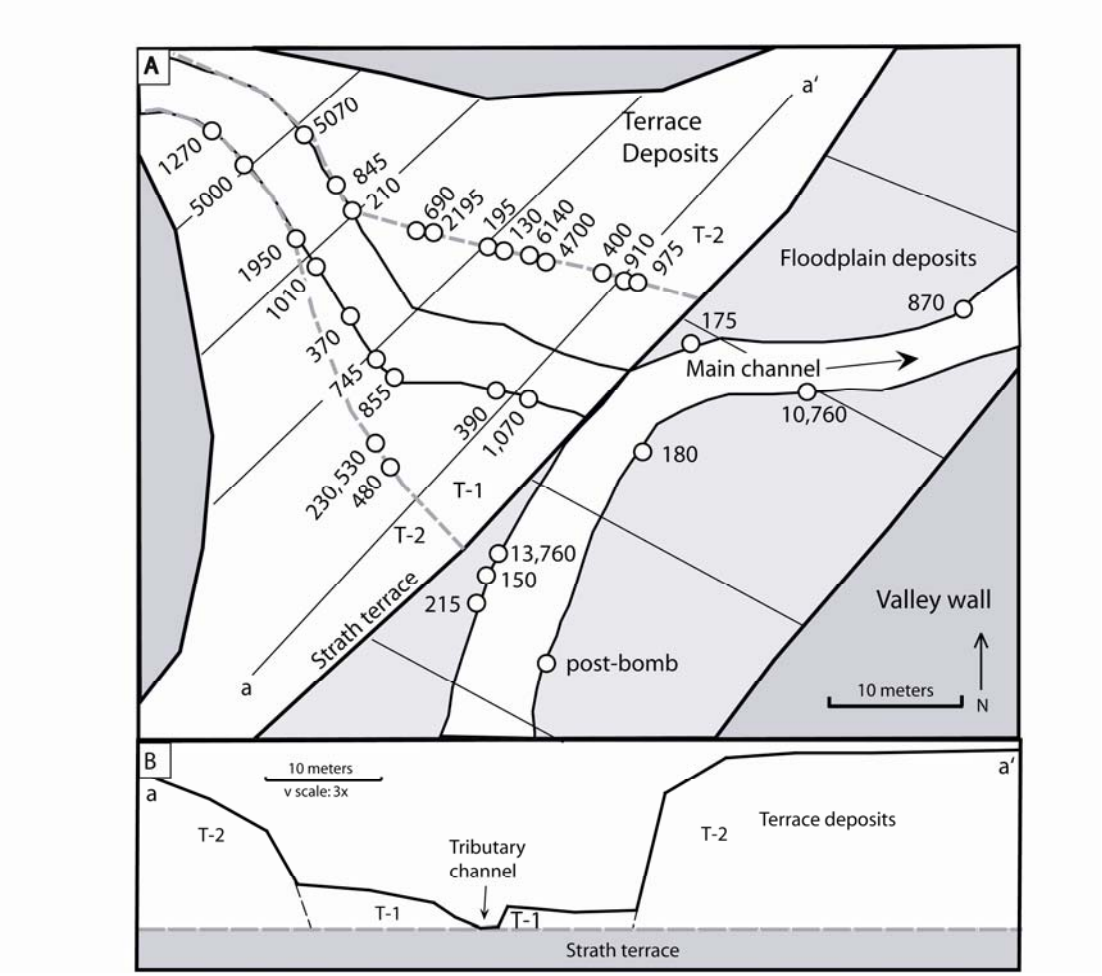

Figure 6. Map of Golden Ridge Creek Site with radiocarbon age estimates. (A) Plan view of Golden Ridge Creek site. Surveyed mainstem and tributary channels and surveyed transects are shown with the locations of sampled deposits. Gray dashed lines indicate T-2 risers. Numbers indicate the raw radiocarbon ages (^{14}C yrs. B.P.). 1σ error is less than 100 ^{14}C yrs B.P. for all age estimates, except for the mainstem ages of 13,790 and 10,760 ^{14}C yrs. B.P. which have errors of 850 and 620 ^{14}C yrs. B.P., respectively (Table 2). (B) Cross section across terrace deposits from a to a'. Black dashed lines represent inferred boundary between T-1 and T-2. Gray dashed lines indicate bedrock elevation.

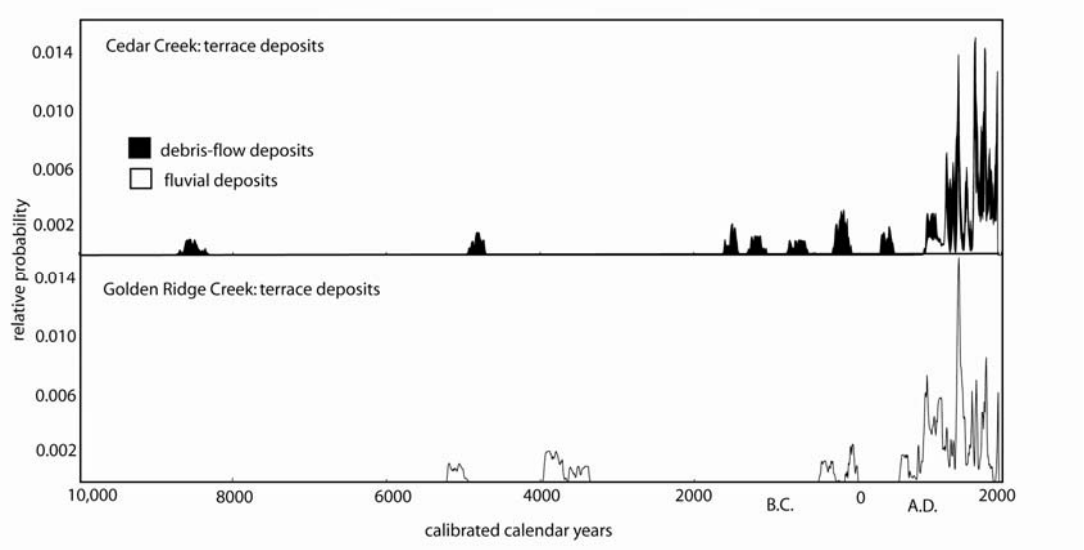

Figure 7. Probability densities of calibrated calendar years for terrace deposits at both sites. Individual probability distributions for each sample are derived from the analysis error and the calibration curves IntCal04 and BombNH04 (Reimer et al., 2004; Hua and Barbetti, 2004). The probability for each date is summed to produce a whole deposit probability spectrum. Debris-flow deposits are filled black and fluvial deposits are white.

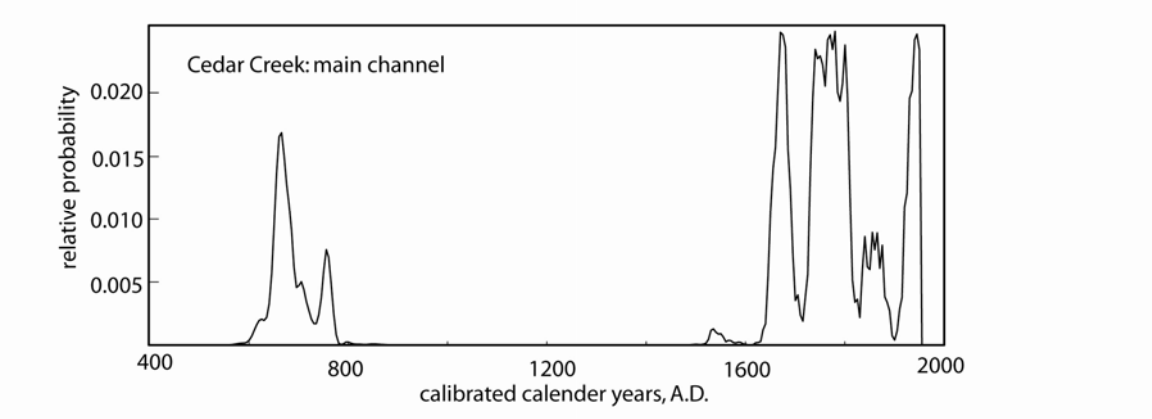

Figure 8. Probability densities of calibrated calendar years for Cedar Creek main channel deposits. Individual probability distributions for each sample are derived from the analysis error and the calibration curves IntCal04 and BombNH04 (Reimer et al., 2004; Hua and Barbetti, 2004). The probability for each date is summed to produce a whole deposit probability spectrum.

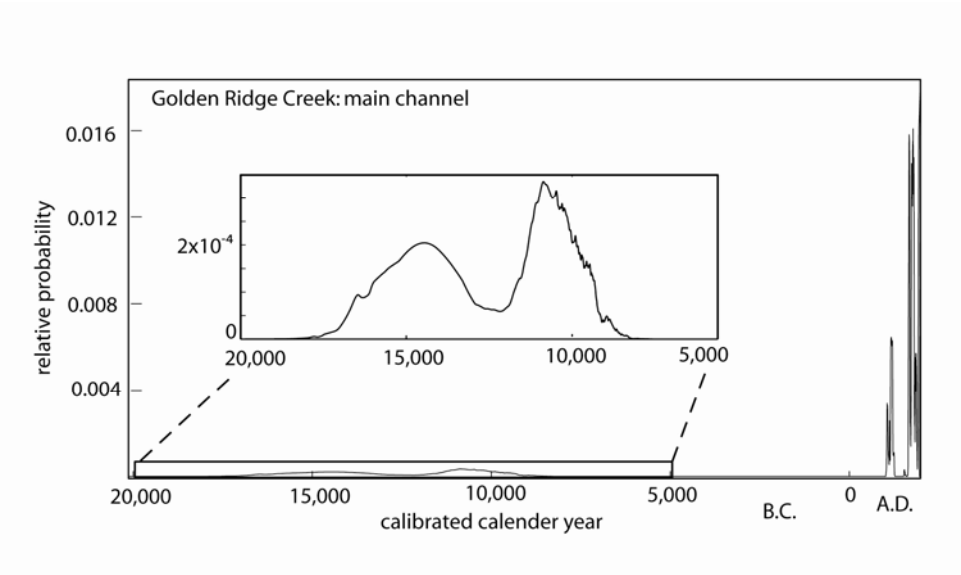

Figure 9. Probability densities of calibrated calendar years for Golden Ridge Creek main channel deposits. Individual probability distributions for each sample are derived from the analysis error and the calibration curves IntCal04 and BombNH04 (Reimer et al., 2004; Hua and Barbetti, 2004). The probability for each date is summed to produce a whole deposit probability spectrum.

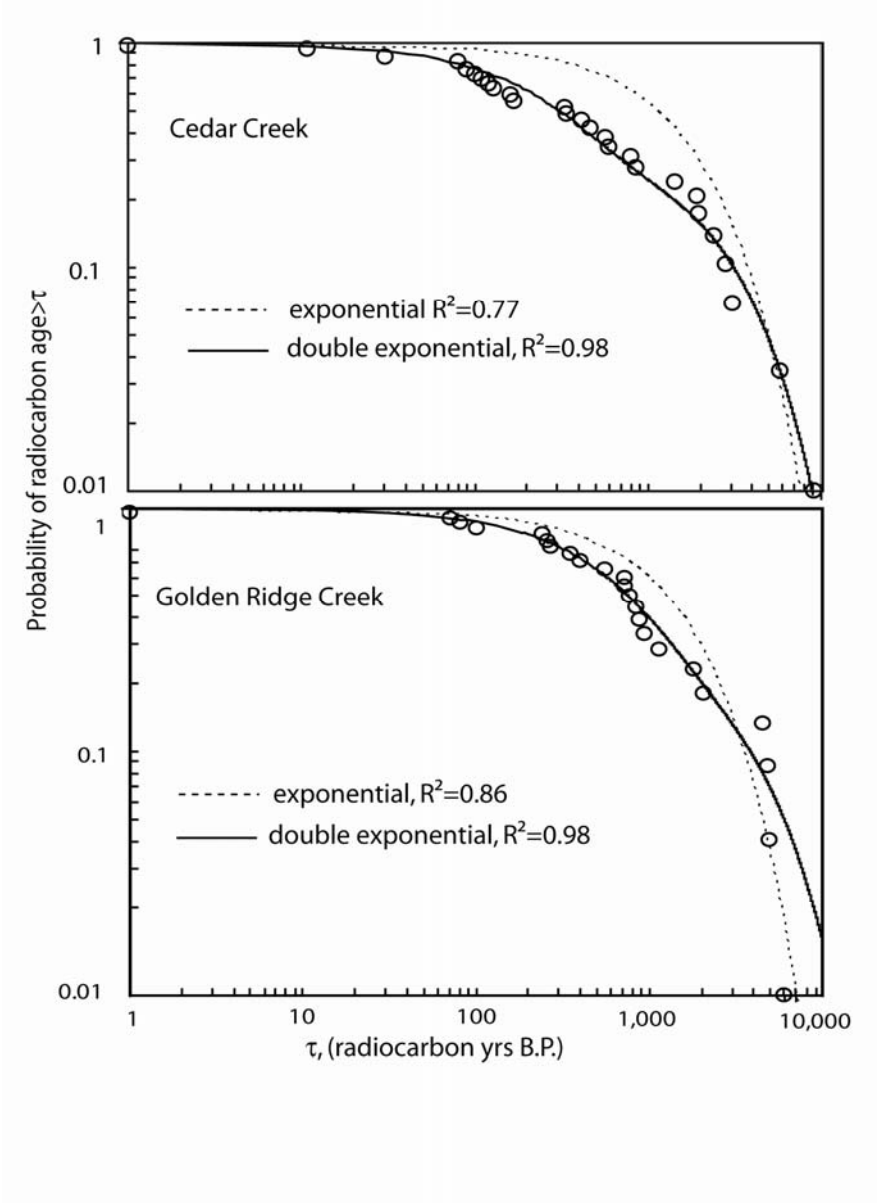

Figure 10. Probability exceedance distributions of the ^{14}C ages for the Cedar Creek and Golden Ridge Creek terrace deposits. Exponential fits to the data are shown with a dashed line, $P(\tau) = e^{-\alpha\tau}$. For Cedar Creek, $\alpha=6.0 \times 10^{-4}$. For Golden Ridge Creek $\alpha=7.0 \times 10^{-4}$. Double exponential fits (solid lines) are given by $P(\tau) = Ae^{-\alpha\tau} + (1-A)e^{-\beta\tau}$. The parameters for Cedar Creek are A= 0.65, $\alpha=4.0 \times 10^{-3}$, $\beta=4.0 \times 10^{-4}$ and for Golden Ridge Creek are A= 0.70, $\alpha=2.0 \times 10^{-3}$, $\beta=3.0 \times 10^{-4}$.

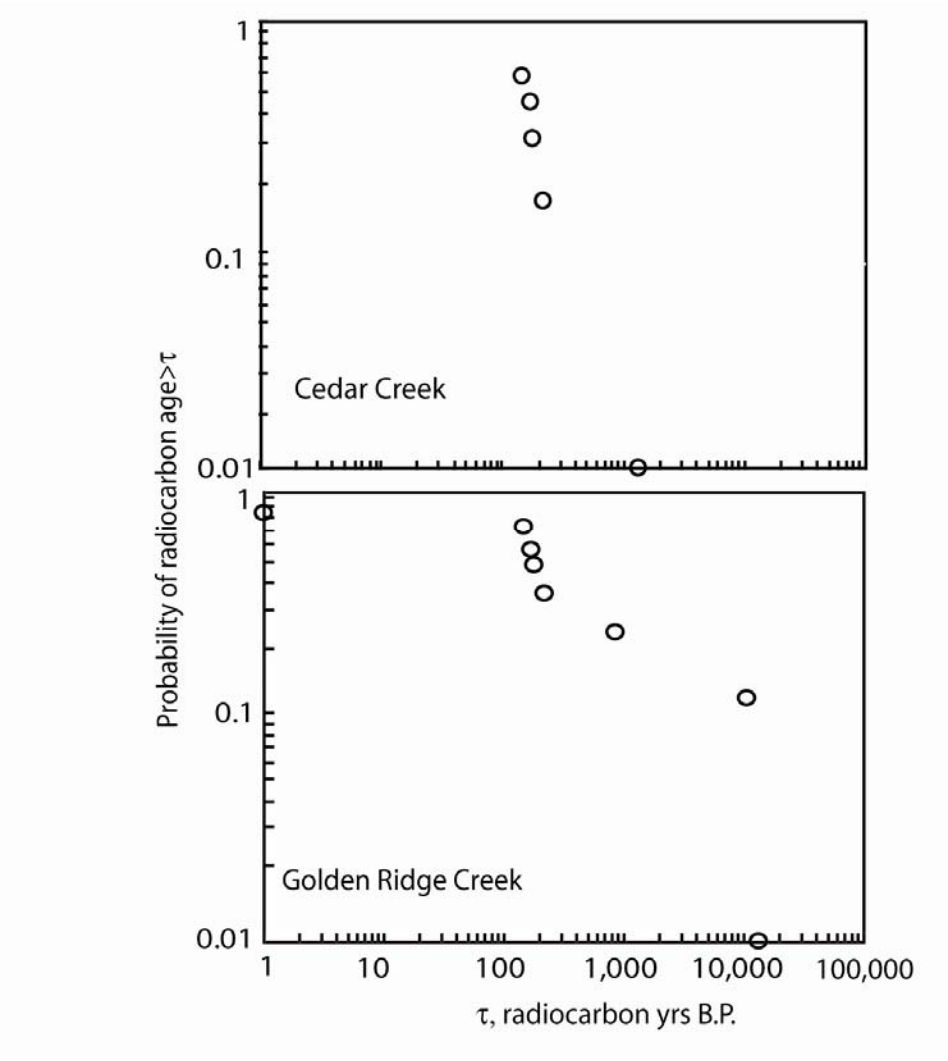

Figure 11. Probability exceedance distributions of the ^{14}C ages for the Cedar Creek and Golden Ridge Creek main channel deposits.

DISCUSSION

Radiocarbon age uncertainty

The radiocarbon age of a charcoal particle in a deposit does not directly represent the timing of the deposition of that deposit. Rather, the age represents the time when the living organism ceased to absorb carbon from the atmosphere (i.e. the time of cell death). Subsequently, a particle may spend time in storage in the tree itself, on a hillslope, in tributary or mainstem channels, or in debris fans or other reservoirs. When evaluating radiocarbon ages, it is difficult to disentangle the amount of time spent in the deposit from which it was sampled and the amount of time the particle spent elsewhere in the reservoir before deposition. The magnitude of inherited age depends on how quickly the particle moved through different basin storage compartments in the basin, and may vary greatly for each sample.

Some attempts have been made to evaluate the age inheritance typically associated with radiocarbon ages. Gavin (2001) estimated typical "inbuilt ages" of soil charcoal to be greater than 180 years, and sometimes on the order of 600 years resulting from the fact that considerable time may elapse between the introduction of atmospheric carbon to the sample and the death of the organism. The inbuilt age only represents the time between the formation of the wood and the fire event that created the charcoal and not the time spent in the watershed before deposition in the feature from which it was sampled.

Some researchers have also investigated the magnitude of inherited age associated with modern deposits. Blong and Gillespie (1978) collected charcoal samples from the mobile bed of a stream in the lower reaches of a 2,000 km^2

catchment in Australia. The bulk radiocarbon ages for different size groups ranged from 600 to 1,600 years B.P., leading the authors to conclude that the age of charcoal in a deposit does not accurately represent the age of modern alluvial deposits. They also found evidence to suggest that the age of charcoal fragments associated with modern deposits increases downstream. Personius (1993) radiocarbon dated a number of detrital charcoal samples from strath terraces in four OCR rivers. Samples from young, modern terraces yielded young ages and prompted the conclusion that inherited age was not a significant problem in that context and radiocarbon samples from older deposits could be interpreted to represent the timing of deposition.

Because it is unlikely that all material is rapidly transported from a tree to the deposit from which it was sampled, the location of the sampled deposits within the basin and potential upstream storage sites must be considered. Also important, the way charcoal is transported through a watershed likely differs from that of bedload transport. Hillslopes and unchanneled hollows serve as primary storage locations for charcoal after a fire event which created the charcoal. Dietrich and Dunne (1978) found that, initially following scour of colluvial hollows, only coarse gravels accumulate until the hollows fill in enough to promote subsurface flow and trap finer material. At this point, the rate of accumulation increases. May and Gresswell (2003) also found that rates of sediment accumulation increased with time since scour, although they attributed that increase to the trapping effect of large woody debris. Hence, sediment stored in hollows has a wide distribution of ages, but that distribution is likely right-skewed, toward younger ages. Reneau and Dietrich (1991) obtained radiocarbon dates in vertical section from OCR hollows exposed in road-

cuts. The radiocarbon ages from these hollows ranged from <200 ^{14}C yrs B.P. at the surface to 10,500 ^{14}C yrs B.P. at the base of hollows. If failure of a colluvial hollow shortly follows a fire event that produced the charcoal, then the residence time of charcoal in the hollows would be very small and much of the charred material delivered by the debris flow would have an age reflecting the timing of the most recent fire event. This material may dominate the age distribution, as it is likely to be the most abundant. Some of the charcoal in a hollow, however, may have been stored there for a long time before evacuation. After hollow failure, debris flows deliver material to tributary channels which may again store charcoal fragments, or transfer them downstream by fluvial processes. Dietrich and Dunne (1978) estimated residence times for material in first, second, and third order tributary channels in the OCR to be 19, 114, and 231 years, respectively. The authors also observed that 50% of the material discharged into tributary channels was delivered as suspended load and was quickly washed out.

Due to the buoyancy of charcoal, a large fraction likely floats out without re-deposition. Another large fraction is probably lost to decay. It seems likely, then, that only relatively small fractions of charcoal move among storage elements so that most charcoal in a deposit is likely to come from events occurring not long before deposition and therefore reflect the time (within bounds established by Gavin, 2001) of that deposition. Figure 12 conceptually summarizes the transport of sediment and charcoal through these basins.

The predominance of ages younger than most of Gavin's (2001) inbuilt ages suggests that most charcoal fragments have not spent much time in upstream storage.

Still, with a large number of samples, the possibility that some samples have substantial inherited ages cannot be ruled out, and with increasing contributing area, the number of upstream storage sites increases. Sampling other landscape elements would help to elucidate the importance of sample reworking in these age data. For instance, dense sampling of recent debris-flow and fluvial deposits would allow characterization of inherited charcoal in deposits formed by these different processes.

The relative positions of the samples highlight cases where significant inherited age is likely. Figures 13 and 14 show the locations of the charcoal samples in the banks marked with the uncalibrated radiocarbon age estimates. Although the random sampling procedure did not typically produce multiple locations in vertical section, there are some instances where samples were taken nearby each other. For example, four samples were taken from the Cedar Creek site at various heights at the same channel distance (at 69 meters: CCF-2, CCF-6, CCF-15, and CCF-16). Samples from 19, 95, 175, and 230 cm above the channel bed have ages of 960, 575, 430, and 190 ^{14}C yrs B.P., respectively. While the diagrams (Figure 13 and 14) are useful for illustrating the relative positions of sample locations throughout the banks, they can be misleading because bank geometries are not well represented. At 65 meters, sample CCF-17 has an age of 235 yrs. B.P. and appears to underlie a sample with an age of 3,235 yrs. B.P (Figure 13). The younger sample was removed from an inset fluvial deposit. At the Golden Ridge Creek site (Figure 14), samples T8-13 and T8-14 at 22 meters have uncalibrated radiocarbon ages of 690 and 2,195 yrs. B.P., respectively. Although these samples are not in exact vertical section, the close proximity of the two samples with such a large difference in age suggests that the

older is inherited charcoal. The Golden Ridge terrace deposits have a contributing area over ten times that of the Cedar Creek fan (Figure 1, Table 1) and therefore have many more potential storage sites upstream, e.g., a series of large, valley-floor debris-flow deposits beginning 300 meters upstream of the tributary junction. The random distribution of samples within the banks and the lack of detailed stratigraphic evidence make it difficult to infer the sequence of depositional events in these tributary deposits. However, the fact that older samples underlie younger in all but one case suggests that the age estimates generally represent the timing of deposition in these deposits.

Transit times

The spatial distribution of radiocarbon age estimates (Figures 13 and 14), attests to the dynamic nature of these tributary deposits and offers clues to the nature of material accretion and removal in these features. Both young and old material are distributed throughout these deposits. If depositional features are accreting, young material might be expected to concentrate at the surface or in the distal portions of the deposit. The mixed assemblage of transit times indicates that these deposits are frequently incised by debris flows and fluvial processes. New material then fills in the accommodation space created by this erosion, thus producing the observed mixed distribution of transit times.

This dynamic character of accretion and erosion suggests that the volumes of these tributary deposits are generally constant over timescales much longer than the time between debris-flow deposition on the fan (the data suggest that the last such deposition occurred about 150 yrs B.P., consistent with the regional fire history of

Impara, 1997). This inference is supported by the abundance of relatively young material, indicating that deposition is actively occurring and the volume of the fan is not shrinking. Also, the fact that these features occupy all of valley accommodation space (from the valley wall to the strath terrace riser) suggests that the size of these deposits is not increasing. The likelihood of a constant volume over long times validates a steady-state assumption and enables analyses of the transit-time distributions and reservoir flux estimates.

The double-exponential shapes of the inferred transit-time distributions provide information about how material moves through tributary confluences to the mainstem channel. The right-skewed distributions suggest that the transfer of material through the tributary deposits to the main channel happens quickly for most material. The "fat-tail" characteristic of the double-exponential highlights the potential for long-term storage. More specifically, the material that is not removed relatively quickly may stay in storage for relatively long times. In eq. (2) the component that moves through quickly is represented by the coefficient A, with a decay scale of α. The material that stays longer (1-A) has transit times long enough to make the average age larger than the mean transit time. Thus the second decay factor, β, is much smaller than α. Stated another way, the inverses of α and β represent the mean transit times through these faster and slower components such that the time $1/\alpha$ is much less than the time $1/\beta$. An analogy for this type of distribution is a reservoir comprised of two populations with different decay rates. In the case of these tributary deposits, the distribution likely indicates that the mechanism of evacuation of fan material favors removal of young material and preservation of older material.

Preferential retention of older material has been observed in other studies that have dated valley floor deposits (Nakamura and Kikuchi, 1997; Lancaster and Casebeer, in press). These studies suggest that material that resides on valley margins is visited by the channel much less frequently and is thus preserved. This mechanism may explain the double-exponential distribution for the Golden Ridge Creek site. At the Cedar Creek fan, material that lies deep in the fan is less likely to be eroded by an incising channel, resulting in the observed transit time distribution.

Mainstem transit times

Because the radiocarbon samples from the mainstem channels are fewer than those from the tributary deposits, a distribution cannot be fit to the dates with confidence. However, these ages do allow comparison between the tributary and mainstem systems. At the Cedar Creek site, the average age of the five radiocarbon samples is 410 ^{14}C yrs B.P., compared to the average age of the fan deposits, 1240 ^{14}C yrs B.P. The lower mainstem average may result from the smaller sample size, but a more likely interpretation is that the difference reflects the relative sizes of the contributing areas and the sampled deposits.

At Golden Ridge Creek, the average ages from the tributary and mainstem deposits are more comparable, 1510 and 1370 ^{14}C yrs B.P., respectively. The two oldest samples (10,760 and 13,790 ^{14}C yrs B.P.) were taken from the mainstem deposits here. Again, the interpretation of these ages is hindered by uncertainty surrounding the timing of the charcoal deposition in these deposits. These samples may indicate long-term storage capability of the contributing basin, which has the

largest contributing area of the four deposits sampled. Another interpretation is that these valley floor deposits are rarely visited by the channel due to the absence of valley-bottom–inundating debris-flow deposits that cause the channel to avulse.

Reservoir Fluxes

This flux analysis helps characterize the role of the tributary deposits in the storage of sediment delivered to the mainstem channel by allowing comparison of basin fluxes to the fluxes through the reservoirs (Table 1). The small deposit volume and relatively large contributing area of the Golden Ridge Creek terrace deposits result in a reservoir flux that is a small fraction of the basin yield. This suggests that most of the material exiting the tributary is not deposited here, and thus these terrace deposits do not play a particularly important role in storage of that tributary's sediment yield.

The calculated flux of material through the Cedar Creek fan is much larger and compares in magnitude to the estimated basin flux. This could only be true if all of the material denuded from the contributing basin ended up in the fan. Suspended and dissolved loads are significant components of denudation (e.g., Dietrich and Dunne, 1978; Larson and Sidle, 1980; Anderson et al., 2002), and are not likely to be stored in the fan. Many of the deposits near the toe of the fan have characteristics of fluvial deposition or reworking. Therefore, one likely explanation for the high reservoir flux is that not all of the material delivered to the fan originates from the tributary but, rather, the mainstem. A comparison of the elevation of high water marks to the height of the terrace suggests that the main channel does occupy the

strath terrace during high flows. While it is likely that mainstem material comprises some portion of the fan, this fraction is probably not large enough to explain the relatively high calculated flux through the fan. The high flux may also be attributed to the steady-state assumptions required for the analysis. If the fan is currently prograding, the flux into the fan would exceed the flux out. This would result in an under-estimation of transit times and thus a high flux rate. However, it appears that the fan is in steady state on the timescale of the mean transit time.

More likely responsible for this high flux rate is that much of the fan volume is comprised of material that is essentially inactive due to burial beneath the typical depth of tributary incision such that, for the purposes of flux estimation, the calculated fan volume is too great. This inactive material is probably not moved through the fan on the same timescale as the active component sampled in this study. The fan volume can be re-estimated to represent only this active material by including only the material above the present depth of tributary incision. With this adjustment the flux through the fan is about 2.10×10^4 kg/yr, roughly two-thirds of the estimated basin yield. Regardless of the exact flux through the debris fan, it is clear that a substantial portion of upstream denudation is stored here. This observation highlights this fan's important role in the storage of sediment at this tributary junction.

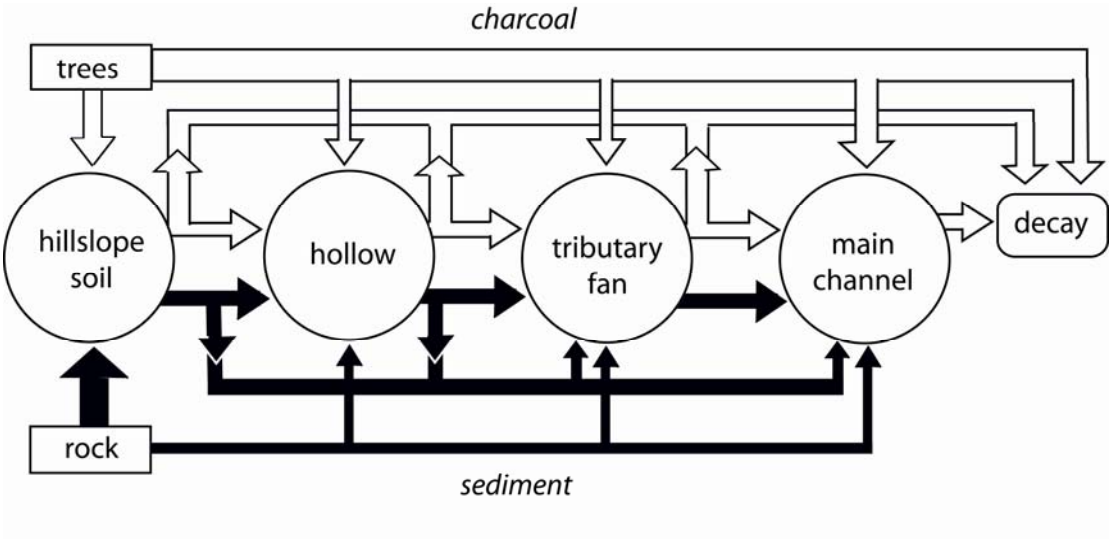

Figure 12. Flow chart illustrating the transport of charcoal and sediment through headwater catchments. Sediment and charcoal originating as rock and trees can be deposited in hillslope soil, hollows, tributary deposits, or mainstem channels and transferred between them. Relative to the amount of charcoal that moves from one storage element to the next, a large fraction will be lost to flushing ("main channel") and decay.

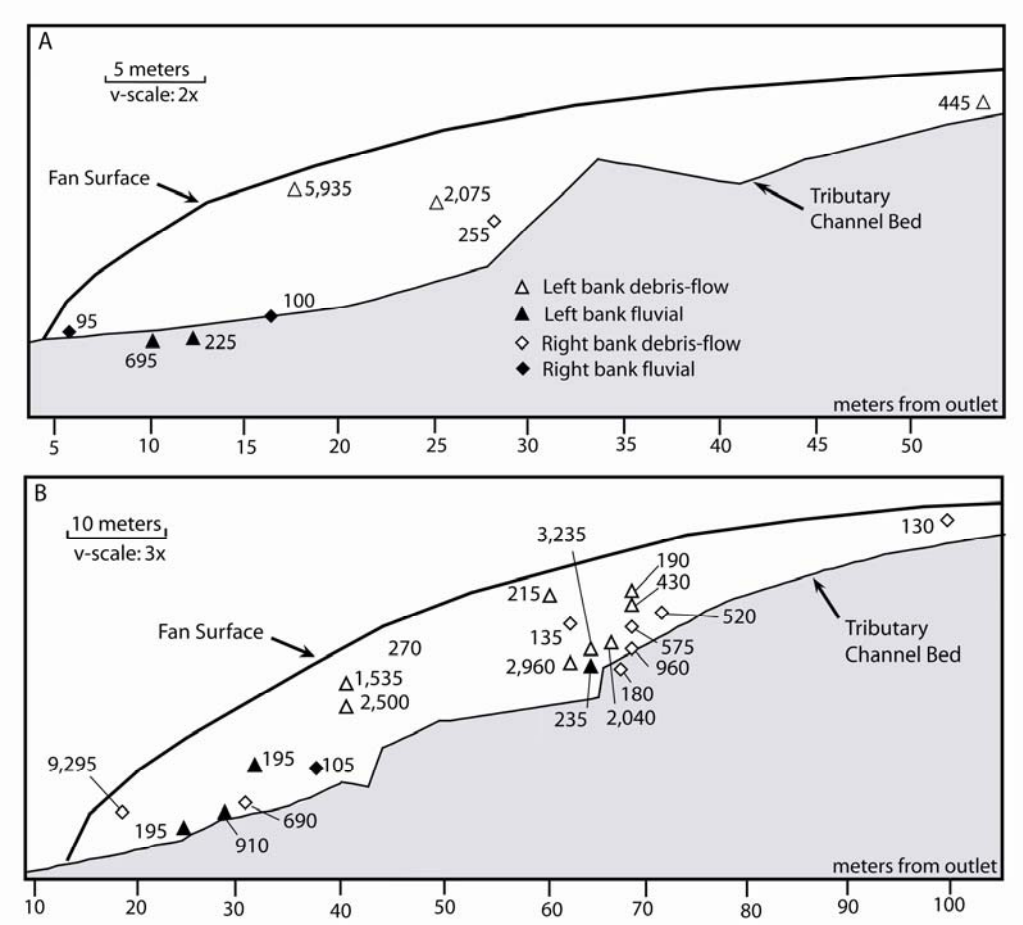

Figure 13. Sample locations within the channel banks at the Cedar Creek Site. Spatial distribution of radiocarbon samples in the lower (A) and upper (B) tributaries. Locations are labeled with ^{14}C age, 1σ error is less than 100 ^{14}Cyears B.P. for all age estimates.

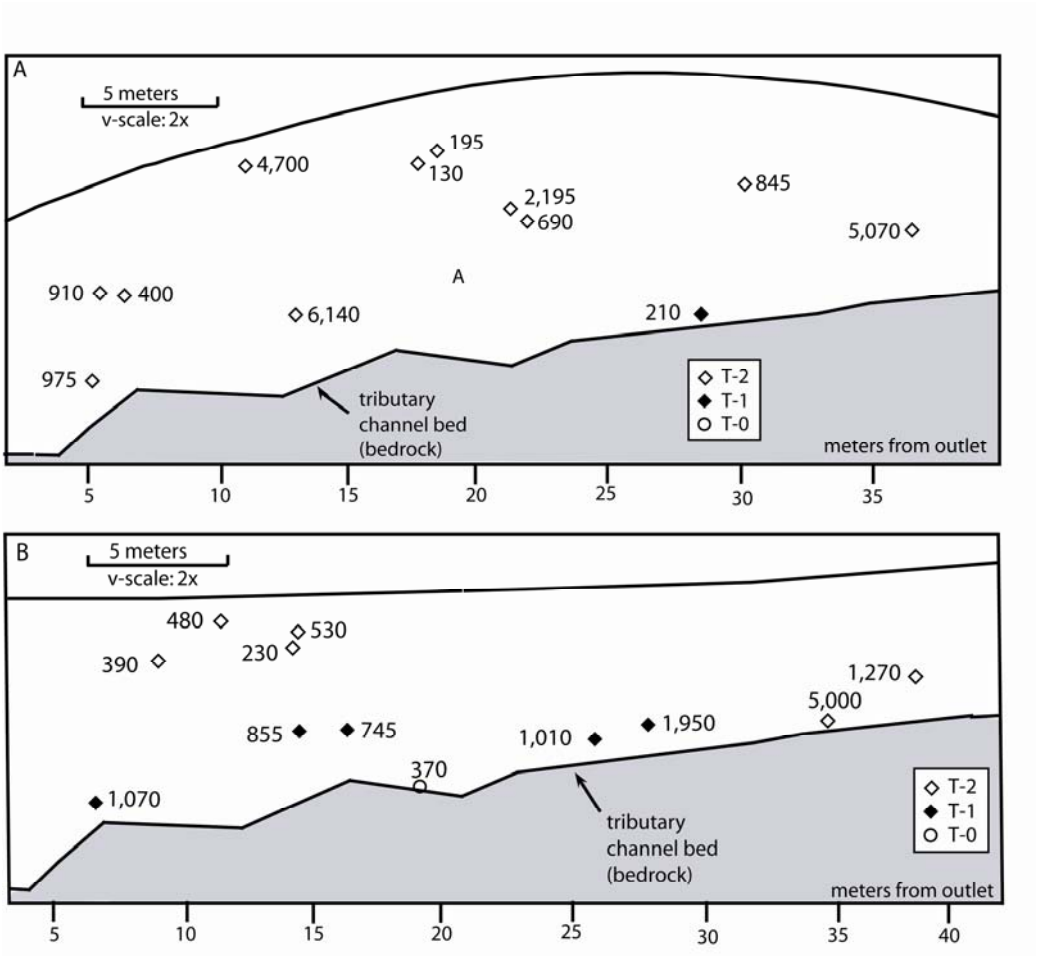

Figure 14. Sample locations within the channel banks at the Golden Ridge Creek Site. Spatial distribution of radiocarbon samples in the left (A) and right (B) banks of the Golden Ridge Creek tributary. Samples are labeled with ^{14}C age, 1σ error is less than 100 ^{14}Cyears B.P. for all age estimates.

CONCLUSIONS

Presented here are 68 radiocarbon ages from two headwater tributary confluences in the OCR. Straightforward interpretation of these data leads to the conclusion that these age estimates capture the transit times of material through these tributary deposits. The double-exponential shape of the inferred transit-time distributions indicates two timescales for the transport of material through these storage reservoirs and implies preferential evacuation of young. The remaining component can persist in storage for millennia buried within debris fans or at valley margins.

At Cedar Creek, the mean transit time through the fan is approximately three times that through the adjacent mainstem deposits. Flux estimates indicate that more than two-thirds of the tributary's sediment yield is stored in this fan. This information and the right-skewed shape of the transit-time distribution indicate that, while much of the basin's sediment is stored in the fan, that storage is temporary and most sediment passes quickly through this dynamic storage reservoir. This large "trapping efficiency" also indicates that such fans serve as important buffers between fish-bearing streams and landscape disturbances (fires, timber harvest) in small watersheds. In contrast, the relatively small reservoir flux of the mainstem and tributary deposits at Golden Ridge Creek indicate their relatively minor roles in the buffering of sediment yields. Still, some long transit times in these reservoirs indicate that these deposits contribute to the long-term persistence of the effects of landscape disturbance in OCR streams.

BIBLIOGRAPHY

Anderson, S.P., W.E. Dietrich, and G.H. Brimhall Jr., 2002, Weathering profiles, mass-balance analysis, and rates of solute loss: Linkages between weathering and erosion in a small, steep catchment: Geological Society of America Bulletin., v. 114, p.1143-1158.

Baldwin, E.M., 1993. Glaciation in the central Coast Range of Oregon: Geology, v. 55. p. 87-89.

Benda, L.E., and T.W. Cundy, 1990, Predicting deposition of debris flows in mountain channels: Canadian Geotechnical Journal, v. 27, p. 409-417.

Benda, L., and T. Dunne, 1997, Stochastic forcing of sediment routing and storage in channel networks: Water Resources Research, v. 33, p. 2865-2880.

Blong, R.J. and Gillespie, R., 1978, Fluvially transported charcoal gives erroneous 14C ages for recent deposits: Nature, v. 271, p. 739-741.

Bolin, B., and Rhode, H., 1973. A note on the concepts of age distribution and transit time in natural reservoirs: Tellus, 25, 58-62.

Bronk Ramsey, C., 2001, Development of the radiocarbon calibration program OxCal: Radiocarbon, v. 43, p. 355-363.

Collinson, J.D., 1978, Alluvial sediments, *in* Sedimentary Environments and Facies. edited by H.G. Reading, pp. 15-60, Blackwell Scientific Publications, Oxford.

Dietrich, W.E., and T. Dunne, 1978. Sediment Budget for a small catchment in mountainous terrain: Zeitschrift fur Geomorphologie, v. 29, p. 191-206.

Dietrich, W.E., Dunne, T., Humphrey, N.F., Reid, L.M., 1982. Construction of sediment budgets for drainage basins, *in* Swanson, F.J., Janda, R.J., Dunne, T., Swanston, D.N. (eds.), Sediment Budgets and Routing in Forested Drainage Basins, Gen. Tech. Rep. PNW-141, pp. 5-23. U.S.D.A. Forest Service, Corvallis, OR.

Eriksson, E. 1971, Compartment models and reservoir theory: Annual Review of Ecology and Systematics, v. 2, p. 67-84.

Gavin, D. G., 2001, Estimation of inbuilt age in radiocarbon ages of soil charcoal for fire history studies: Radiocarbon, v. 43, p. 27-44.

Gilbert, G. K. 1877, Report on the Geology of the Henry Mountains. United States Geographical and Geological Survey of the Rocky Mountain Region.

Hack, J. T. 1960. Interpretation of erosional topography in humid temperate regions: American Journal of Science v. 258A p. 80-97.

Hancock, G.S., and Anderson, 2002, Numerical modeling of fluvial strath-terrace formation in response to oscillating climate: Geological Society of America Bulletin, v. 114, p. 1131-1142.

Heimsath, A.M., W.E. Dietrich, K. Nishiizumi, and R.C. Finkel, 2001. Stochastic processes of soil production and transport: erosion rates, topographic variation, and cosmogenic nuclides in the Oregon Coast Range: Earth Surface Processes and Landforms, v. 26, p. 531-552.

Heller, P.L., and Dickinson, W.R., 1985. Submarine ramp facies model for delta-fed, sand-rich turbidite systems: American Association of Petroleum Geologists Bulletin, v. 69 , p.960-976.

Hoadley, R.B., 1990, Identifying Wood: Accurate Results with Simple Tools. The Taunton Press, Newtown CT.

Hua, Q. and M. Barbetti, 2004, Review of trophospheric bomb C-14 data for carbon cycle modeling and age calibration purposes: Radiocarbon, v. 46, p.1273-1298.

Impara, P., 1997, Spatial and Temporal Patterns of Fire in the Forests of the Central Oregon Coast Range: Ph.D. dissertation, Oregon State University, Corvallis, 354. p.

Iverson, R. M. 1997. The physics of debris flows, Reviews of Geophysics: v. 35, p. 245-296.

Iverson, R. M., Reid,M. A., and LaHusen, R. G., 1997, Debris-flow mobilization from landslides: Annual Review of Earth and Planetary Sciences, v. 25, p. 85–138.

Lancaster S.T. and Casebeer, N.E., Sediment storage and evacuation in headwater valleys at the transition between debris-flow and fluvial processes: Geology, in press.

Lancaster, S.T., and G.E. Grant, 2006, Debris dams and the relief of headwater streams: Geomorphology, v. 82 (special issue on bedrock rivers, edited by P.A. Carling), p. 84-97.

Lancaster, S.T., S.K. Hayes, and G.E. Grant, 2003, Effects of wood on debris flow runout in small mountain watersheds, Water Resources Research, v. 39.

Lancaster, S.T., S.K. Hayes, and G.E. Grant, 2001, Modeling sediment and wood storage and dynamics in small mountainous watersheds, in Geomorphic Processes

and Riverine Habitat, J.M. Dorava, D.R. Montgomery, B.B. Palcsak, and F.A. Fitzpatrick (eds.), p. 85-102, American Geophysical Union, Washington.

Larson, K.R. and Sidle, R.C., 1980, Erosion and sedimentation data catalog of the Pacific Northwest: Portland, Oregon, USDA Forest Service, Pacific Northwest Region, Report No. R6-WM-050–1981, 73 p.

Major, J.J., 1997, Depositional processes in large-scale debris-flow experiments: The Journal of Geology, v. 105, p. 345-366.

Malmon, D.V., Dunne, T. and Reneau, S.L., 2003, Stochastic theory of particle trajectories through alluvial valley floors: The Journal of Geology, v. 111, p. 525–542.

May, C.L., and Gresswell, R.E., 2004, Spatial and temporal patterns of debris-flow deposition in the Oregon Coast Range, USA: Geomorphology, v. 57, p. 135–149.

May, C.L., and Gresswell, R.E., 2003, Processes and rates of sediment and wood accumulation in headwater streams of the Oregon Coast Range, USA: Earth Surface Processes and Landforms, v. 28, p. 409-424.

Meyer, G.A., S.G. Wells, and A.J.T. Jull, 1995. Fire and alluvial chronolgy in Yellowstone National Park: Climatic and intrinsic controls on Holocene geomorphic processes, Geological Society of America Bulletin., v. 107, p. 1211-1230.

Montgomery, D. R., Schmidt, K. M., Greenberg, H., and Dietrich, W. E., 2000, Forest clearing and regional landsliding: Geology, v. 28, p. 311-314.

Montgomery, D.R. and W.E. Dietrich, 1994, A physically based model for the topographic control on shallow landsliding: Water Resources Research, v. 30, p.1153-1171.

Nakamura, F., and Kikuchi, S., 1996, Some methodological developments in the analysis of sediment transport processes using age distribution of floodplain deposits: Geomorphology, v. 16, p. 139–145.

Personius, S.F., 1993, Age and Origin of Fluvial Terraces in the Central Coast Range, Western Oregon, U.S. Geological Survey Bulletin No. 2038.

Personius, S.F., H.M. Kelsey, and P.C. Grabau, 1993. Evidence for regional stream aggradation in the central Oregon Coast Range during the Pleistocene-Holocene transition: Quaternary Research, v. 40, p. 297-308.

Reneau, S.L., and Dietrich, W.E., 1991, Erosion rates in the southern Oregon Coast Range: Evidence for an equilibrium between hillslope erosion and sediment yield: Earth Surface Processes and Landforms, v. 16, p. 307-322.

Reneau, S.L., and Dietrich, W.E., 1990, Depositional history of hollows on steep hillslopes, coastal Oregon and Washington: National Geographic Research, v. 6, p. 220-230.

Reneau, S.L., W.E. Dietrich, M. Rubin, D.J. Donahue, and A.J.T. Jull 1989. Analysis of hillslope erosion using dated colluvial deposits: The Journal of Geology. v. 97, p. 47-63.

Reeves, G.H., P.A. Bisson, and J.M. Dambacher, 1998. Fish communities, *in* River Ecology and Management: Lessons from the Pacific Coastal Ecoregion, ed. By R.J. Naiman and R.E. Bilby, pp. 200-234, Springer-Verlag, New York.

Reimer, P.J., M.G.L. Baillie, E. Bard, A. Bayliss, J.W. Beck, C.J.H. Bertrand, P.G. Blackwell, C.E. Buck, G.S .Burr, K.B. Cutler, P.E. Damon, R.L. Edwards, R.G. Fairbanks, M. Friedrich, T.P. Guilderson, A.G. Hogg, K.A. Hughen, B. Kromer, G. McCormac, S. Manning, C. Bronk Ramsey, R.W. Reimer, S. Remmele, J.R. Southon, M. Stuiver, S. Talamo, F.W. Taylor, J. van der Plicht and C.E. Weyhenmeyer, 2004, IntCal04 terrestrial radiocarbon age calibration, 0-26 cal kyr BP: Radiocarbon, v. 46, p. 1029-1058.

Sklar L. and W.E. Dietrich, 1998, River longitudinal profiles and bedrock incision models: Stream Power and the influence of sediment supply, *in* Rivers Over Rock: Fluvial Processes in Bedrock Channels, Geophys. Monogr. Ser., v. 107, edited by K.J. Tinkler and E.E. Wohl, , American Geophysical Union, Washington, D.C., p. 237-260.

Stock, J., and W. E. Dietrich, 2003, Valley incision by debris flows: Evidence of a topographic signature: Water Resources Research., v. 39, p. 1089.

Suwa, H. and S. Okuda, 1983. Deposition of debris flows on a fan surface Mt. Yakedake, Japan: Zeitschrift fur Geomorphologie v. 46. p. 79-101.